

Supporting Information

Phosphorus-Doped TiO₂ Nanotube Arrays for Visible-Light-Driven Photoelectrochemical Water Oxidation

Dong-Dong Qin,^{*a} Qiu-Hong Wang,^a Jing Chen,^a Cai-Hua He,^a Yang Li,^a Cai-He Wang,^a Jing-Jing Quan,^a Chun-Lan Tao^{*b} and Xiao-Quan Lu^{*a}

^a*Key Lab of Bioelectrochemistry and Environmental Analysis of Gansu, College of Chemistry and Chemical Engineering, Northwest Normal University, Lanzhou, Gansu 730070, People's Republic of China.*

^b*School of Physical Science and Technology, Lanzhou University, Lanzhou, Gansu 730000, People's Republic of China.*

Corresponding author: E-mail: qindd05@gmail.com (D. D. Qin), taochl@lzu.edu.cn (C. L. Tao), luxq@nwnu.edu.cn (X. Q. Lu)

1. Experimental:

1.1 Chemicals

All the chemicals including high purity Ti foils (99.6% purity, thickness of 0.2 mm, Aesar Chemical Co. Ltd.), ammonium fluoride (NH₄F, Aldrich, ≥99.6%), ethylene glycol (Aldrich, ≥99.0%), ethanol (Aldrich, ≥99.7%); NaOH (Aladdin, ≥96%); sodium hypophosphite (NaH₂PO₂·H₂O, Aldrich, ≥99.0%) were used as received without further purification. All aqueous solutions were prepared in deionized (DI) water with a resistivity of 18.25 MΩ·cm.

1.2 Equipments and measurements

The morphology of samples were characterized by using a field-emission scanning electron microscope (Zeiss ULTRA Plus) operated at an accelerating voltage of 5 kV. X-ray diffraction patterns (XRD) were recorded on a PANalytical X'Pert PRO instrument using Cu Kα radiation (40 kV, λ = 1.5406 Å) between 20° to 80° at a scanning rate of 0.067°/s. Raman spectra were measured at a JY-HR800 Micro-Raman, using a 532 nm wavelength YAG laser with a laser spot diameter of about 600 nm. TEM images were obtained using a JEM-1200EX FEI microscope. UV-visible diffuse reflectance spectra were measured on a UV-2550 (Shimadzu) spectrometer

by using Ti foil as the reference. The elemental composition was determined by X-ray photoelectron spectroscopy (Kratos Axis Ultra DLD). Photoelectrochemical measurements were made in 1 M NaOH under AM 1.5G illumination ($100 \text{ mW}\cdot\text{cm}^{-2}$) in a three-electrode configuration with TiO_2 nanotube arrays as working photoelectrode, saturated calomel electrode (SCE) as reference electrode, and platinum foil as counter electrode. Sunlight was simulated with a 300W Xenon lamp and an AM 1.5G filter (Newport). The light intensity was set using a calibrated crystalline silicon solar cell. Photocurrent response, open circuit voltage decay and electrochemical impedance spectroscopy (EIS) were recorded using a CHI-660D potentiostat. The impedance data was fit to an equivalent circuit model using Zview software. During measurements for Mott-Schottky plots, the superimposed alternating current (AC) signal was maintained at 5 mV, with frequency of 100 Hz and potentials between -0.3 and 1.0 V versus RHE in the dark in an electrolyte of 1 M NaOH, with Pt as the counter electrode and saturated calomel electrode(SCE) as the reference electrode. The capacitance was extracted from the EIS spectra by use of an equivalent circuit $R_s(\text{CPE}-R_p)$, where R_s is the ohmic contribution, CPE is a constant phase element that takes into account non-idealities in the capacitance of the Helmholtz layer, and R_p is the charge-transfer resistance. For EIS testing, a fixed bias potential of 1.5 V vs RHE was used and the light intensity was set to $100 \text{ mW}\cdot\text{cm}^{-2}$. The intensity modulated photocurrent spectroscopy (IMPS) response was measured using the light source of a LED array (470 nm) driven by the output current of the Autolab LED Driver. The dc output of the LED Driver was controlled by the DAC164 of the Autolab, and the ac output of the LED Driver was controlled by the FRA32 M module. The ac amplitude was set to 25% of the dc output. The IMPS response was examined over a frequency range from 0.1 Hz to 10 kHz at an applied potential of 1.23 V vs RHE in 1.0 M NaOH solution. The transfer function, H, was monitored using the external inputs of the FRA module. The potentials of the photoelectrodes are reported against RHE, converting between the SCE and RHE potential scales using $E_{RHE} = E_{SCE} + 0.059\text{pH} + E_{SCE}^0$, where pH is 13.6 (1.0 M NaOH) and $E_{SCE}^0 = 0.2415$

V (25 °C).

1.3 Synthesis of pristine and P-doped TiO₂ nanotube arrays

Titanium foil with size of 1.5 × 2.5 cm were completely washed successively by water, acetone and ethanol in an ultrasonic cleaner, and finally dried in a vacuum oven at 30 °C. The anodization was performed at 50 V in a two-electrode electrochemical cell for variable time (3, 5, 7, 8, 10 and 15 h, respectively) with a platinum foil as the counter electrode. Anodization electrolyte was composed of 0.3 wt% NH₄F and 3.0 wt% H₂O in ethylene glycol. The as-prepared nanotube samples were annealed at different temperature for 2 h in a tube furnace with heating rate of 1 °C/min. PH₃ was generated by thermal decomposition of sodium hypophosphite hydrate (NaH₂PO₂·H₂O) at 300 °C, and reacted with annealed TiO₂ nanotubes at the same temperature for 1 h in a tube furnace under a constant N₂ flow.

Fig. S1

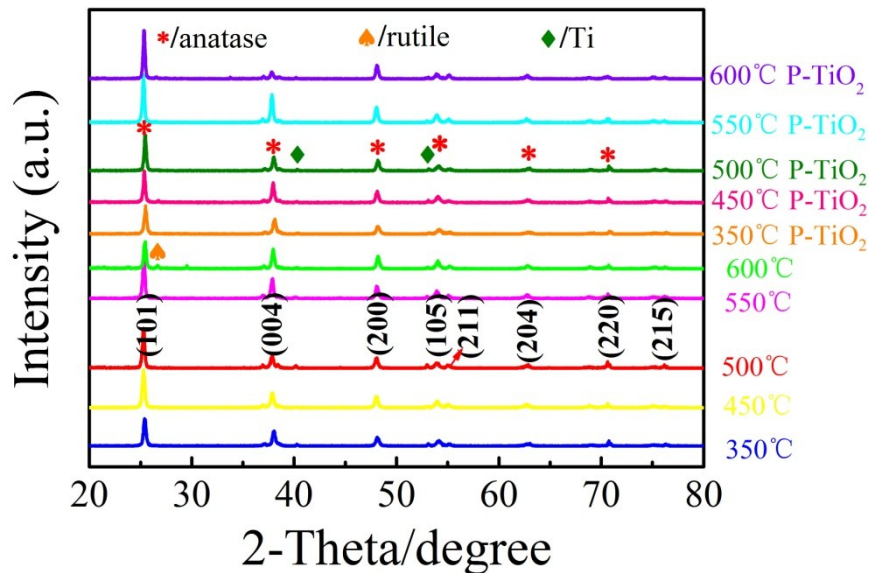


Fig. S1 XRD diffraction patterns of the samples.

Fig. S2

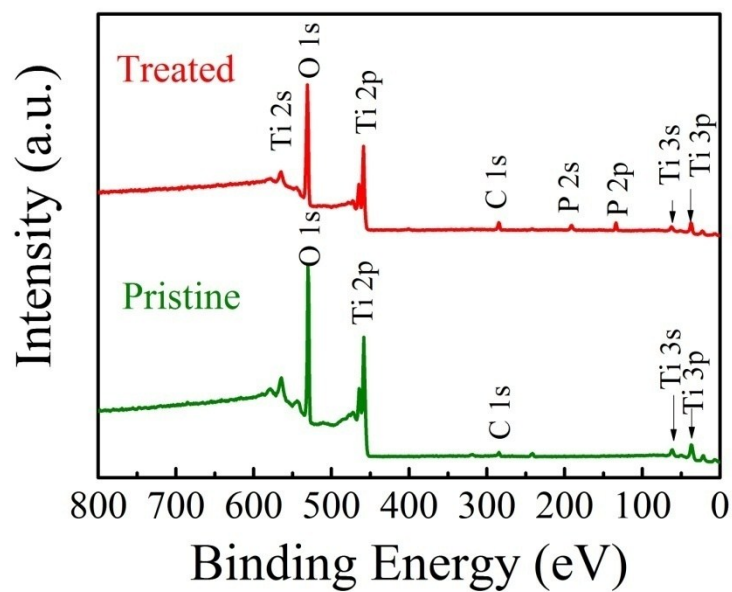


Fig. S2 XPS survey of undoped (pristine) and P-doped (treated) TiO₂ nanotube arrays.

Fig. S3

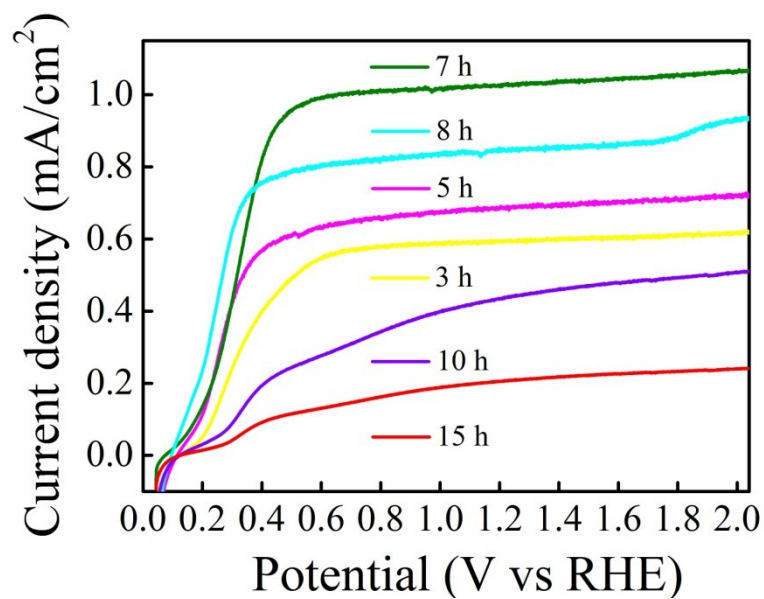


Fig. S3 Photocurrent of TiO₂ nanotube arrays with different anodization time, annealed at 500 °C in air.

Fig. S4

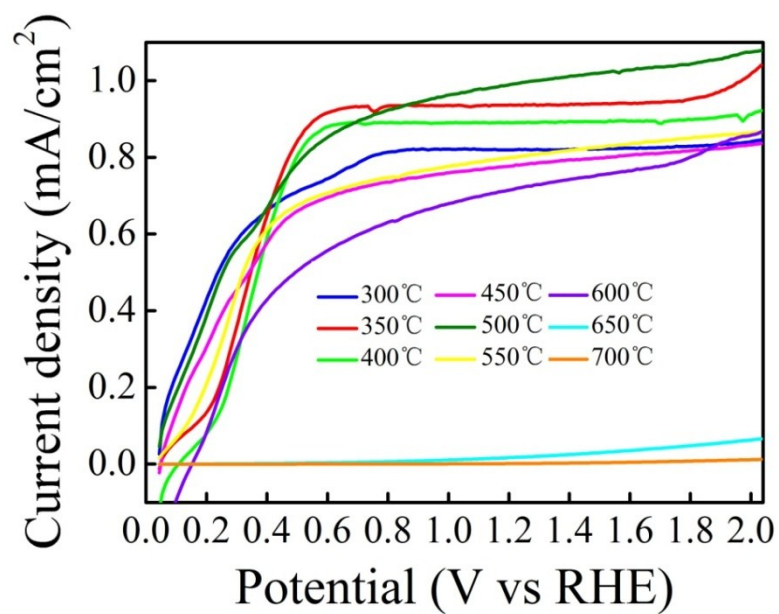


Fig. S4 Photocurrent of 7 h TiO₂ nanotube arrays after annealing at different temperature in air.

Fig. S5

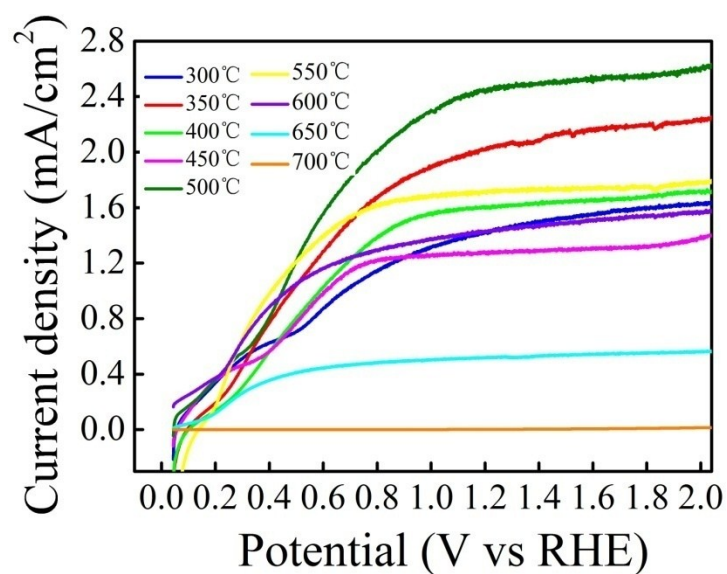


Fig. S5 Photocurrent of annealed 7 h TiO₂ nanotube arrays after annealing at 300 °C in PH₃ atmosphere for 1 h

Fig. S6

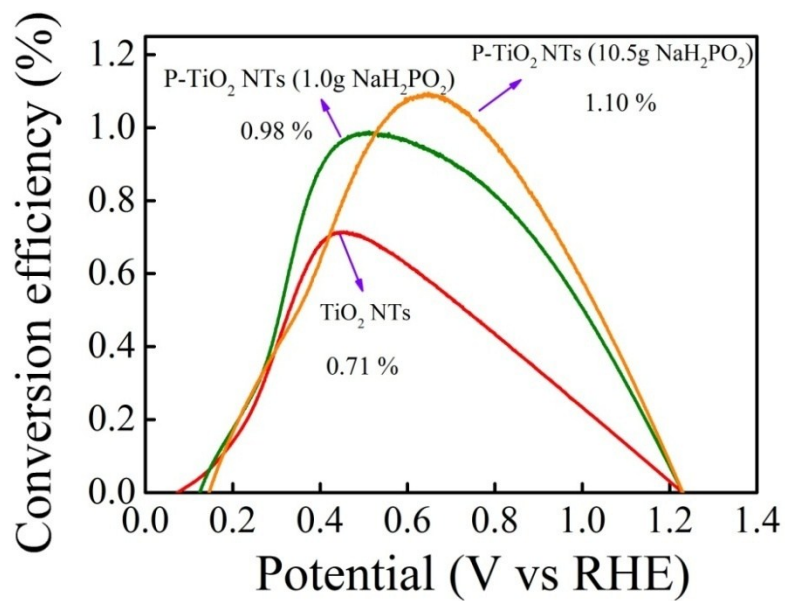


Fig. S6 Photoconversion efficiency of the samples.

Fig. S7

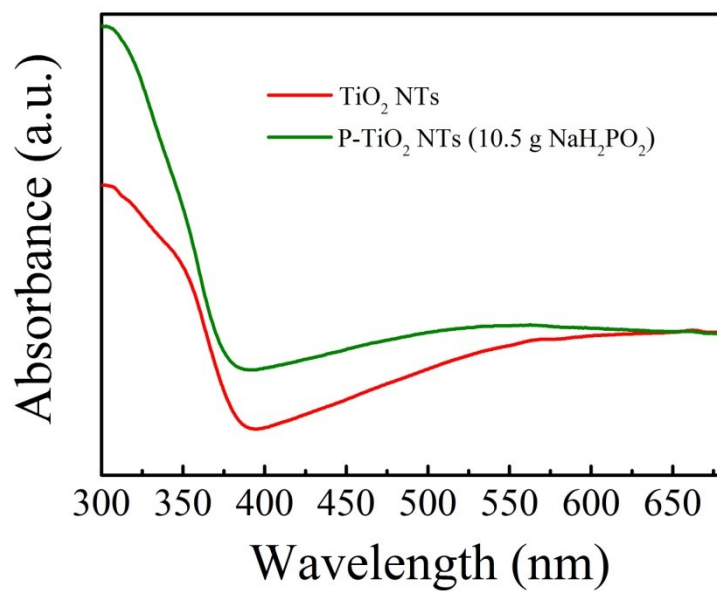


Fig. S7 Optical spectra of the samples.

Fig. S8

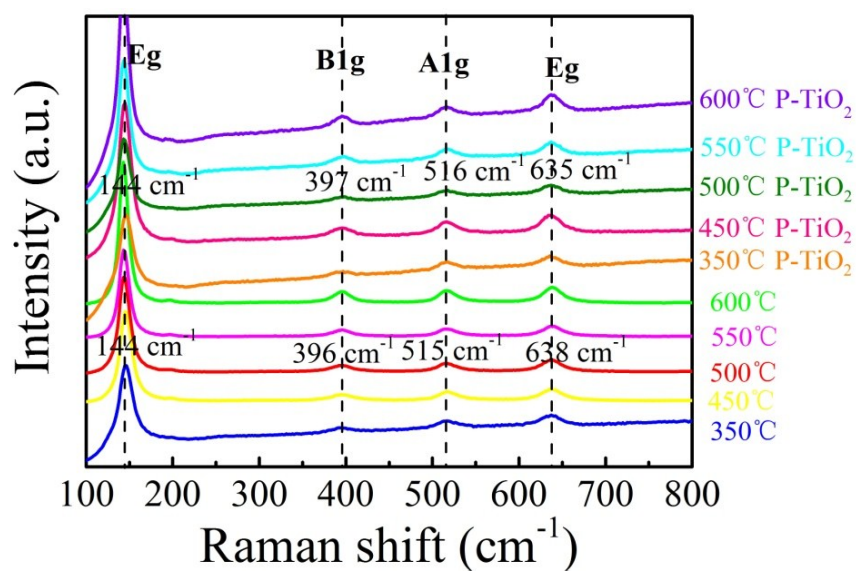


Fig. S8 Raman spectra of the samples.

Fig. S9

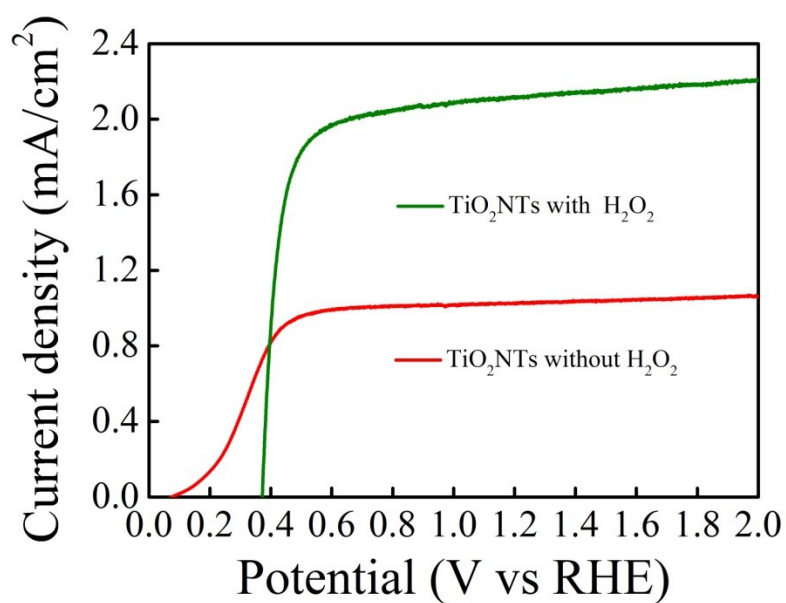


Fig. S9 Photocurrent of undoped TiO₂ nanotube arrays with and without H₂O₂.

Fig. S10

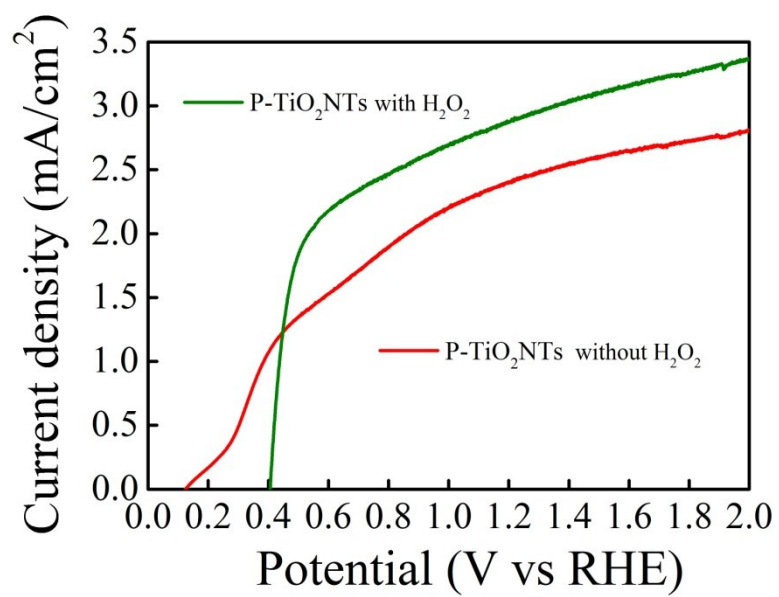


Fig. S10 Photocurrent of P-doped TiO₂ nanotube arrays with and without H₂O₂.